Supporting Information

Fagegaltier et al. 10.1073/pnas.0809208105

SI Text

Suppressor Transgenic Constructs. B2 and P19 cDNA was amplified by PCR from pBWDi-FHV-B2 (B2 Swiss-Prot P68831 sequence) and pBIN-P19 (1), respectively, using the primers B2-F CACCATGCCAAGCAAAC, B2-R CAGTTTTGCGGGTGG, P19-F 5′-CACCATGGAACGAGC-3′ and P19-R CTCGCTTTCTTTTTCG, and cloned into the *p*-ENTR-D-TOPO vector (Invitrogen) to give pENTR-B2 and pENTR-P19, respectively. For pENTR-NLS-P19 construct, the nuclear localization sequence was amplified from the transformer cDNA using the primers tra-F CACCATGAGGCACAGAAGGCATCGCCA and tra/P19-R GCTCGTTCCATTCGTTCACTGCTG on one hand, and P19 was amplified from pENTR-P19 using the primers tra/P19-F CAgCAgTgAACgAATggAACgAgC and P19-R CTCGCTTTCTTTTTCG however. Both PCR products were purified, used in a mix as templates in a second PCR step using the external primers tra-F and P19-R. The traNLS-P19 PCR product was then cloned into *p*-ENTR-D-TOPO. pENTR-B2, pENTR-P19 and pENTR-NLS-P19 were recombined into the pUASp vector (2) adapted for the Gateway system (*Drosophila* Gateway Vector collection, Carnegie Institution) to give C-terminal FLAG tagged pPWF-B2, pPWF-P19 and pPWF-NLS-P19 constructs, respectively. The sequences of these constructs were verified by sequencing before establishing transgenic stocks by standard injection procedure. For expression in S2 cells, viral protein genes from *p*-ENTR-B2, pENTR-P19, and pENTR-NLS-P19 plasmids were recombined into the copper inducible pMT-DEST48 Gateway vector (Invitrogen) to produce V5 tagged protein, or into the pAWH destination vector (*Drosophila* Gateway Vector collection, Carnegie Institution) to produce HA tagged protein under the control of the Act5C promoter.

Genetic Crosses. To analyze the effect of suppressors on *white* RNAi, we constructed an homozygous *w1118*, GMR>IR[w]; GMR>GAL4 stock by genetic recombination and crossing, and crossed it to homozygous UAS>GFP, UAS>B2, UAS>P19 and UAS>NLS-P19 lines. For controls, the same lines were crossed to the homozygous *w1118;* GMR>GAL4 stock.

To analyze the effect of suppressors on *EcR* RNAi, we constructed a w^{1118}; GMR>GAL4, UAS>IR[EcR] / *CyO* stock by genetic recombination and crossed it to the UAS>GFP, UAS>B2, UAS>P19 and UAS>NLS-P19 lines. To analyze the effect of suppressors of bantam silencing, we recombined the *Tubulin*>GFP-ban sensor transgene with the *engrailed*>GAL4 driver on the third chromosome and crossed the resulting homozygous stock to the UAS>B2, UAS>P19, and UAS>NLS-P19 lines

To analyze the effect of mutations on white PEV, homozygous *ln (1)*w^{m4h} (w^{m4}) females carrying the mutant allele over the *CyO Act5C*>*GFP* or *TM6B Tb* balancer chromosome were crossed to males carrying the mutant allele in a w^{1118} background, and effects in male offspring was addressed (see Fig. S7 for the design of genetic tests).

Sb^V variegation was analyzed by crossing *T(2;3)*Sb^V, *In(3R)Mo*, Sb^1 *sr1/TM3 Ser* females to heterozygous mutant males over a balancer or homozygous $dcr2^{R496X}$, $dcr2^{L811fsX}$, or $ago2^{414}$ mutant males. In the *Stubble-variegator* translocation Sb^V, the Sb^1 dominant mutation becomes silenced by pericentric heterochromatin (2R), resulting in composite bristle length. A strong suppressor or enhancer will give nearly all stubble or wild-type bristles, respectively. The length of seven pairs of major dorsal macrochaetes was examined as described in ref. 3 and attributed a wild type or *Stubble* (*Sb*) score. At least 30 flies of each sex were examined in a given cross. For viral proteins effects, bristles were scored in the offspring of *T(2;3)*Sb^V, *In(3R)Mo*, Sb^1 *sr1/TM3* males crossed to (1) *Act5C*-GAL4 control driver, (2) *Act5C*-GAL4>*B2*, (3) *Act5C*-GAL4>*P19* or (4) *Act5C*-GAL4>*NLS-P19* females.

Eye Pigment Determination. Assays were performed on same aged 3-day-old virgin females. Five heads per genotype were manually collected and homogenized in 50 μl of a freshly prepared solution of acidified methanol (0.1% HCl). Pigment was extracted by rocking tubes for 36 h at 4 °C. Homogenates were then incubated at 50 °C for 5 min, clarified by centrifugation and optical density of each sample was read at 480 nm. Three independent extractions were performed for each genotype, and the mean values of the absorption per extraction were calculated.

Salivary Gland Immunostaining. B2, P19 or NLS-P19 homozygous transgenic lines were crossed to the *lio*>GAL4 driver line. Salivary glands from third instar wandering larvae were dissected in PBS, fixed for 30 min in PBST (PBS-0.1% Triton X-100) containing 3.7% formaldehyde, rinsed twice in PBST and blocked for 30 min in PBST, 1% BSA, 10% FBS. Samples were incubated with mouse anti-FLAG M2 antibodies (1:500). We used secondary FITC-coupled anti-mouse antibodies (1:500). Whole salivary glands were mounted in DAPI containing Vectashield (Vector Labs) and analyzed using confocal Leica TCS LPE microscope.

Immunofluorescence on S2 Cells. Cells transfected with 2 μg of pMT-DEST48, pMT-B2, pMT-P19 or pMT-NLS-P19 plasmid and induced as below were washed once in PBS, gently spun on slides, and immediately fixed for 10 min in 3.6% formaldehyde. The slides were then rinsed three times in PBS, and cells permeabilized for 10 min in 4× SSC, 0.1% Triton, 0.1% Tween-20 before blocking in the same buffer containing 5% BSA. Mouse anti-V5 antibody (1:500, Invitrogen) was incubated overnight in blocking buffer, and detected with Cy3-anti-mouse secondary. Slides were mounted in DAPI containing Vectashield and viewed under a fluorescence microscope attached to an Axioplan imaging Apotome apparatus (Zeiss).

Immunoprecipitation from S2 Cells. For transient expression, 4 μg of pMT-DEST48 control plasmid, pMT-B2-V5, pMT-P19-V5, or pMT-NLSP19 were transfected in S2 cells with Effecten Reagent (Invitrogen) according to the manufacturer's instructions. Two days after transfection, cells were split and cultured for two more days. Each well was then induced with 500 μM CuSO4, and cells were harvested 20 h after induction. For total RNA analysis, cells were pelleted and RNA extracted with TRIzol Reagent (Invitrogen) according to the manufacturer's instructions, except that RNA washes were performed in 80% ethanol. For immunoprecipitation experiments, cells were harvested, washed twice in PBS, and lysed on ice for 30 min in Lysis buffer (50 mM Tris·HCl pH7.5, 150 mM NaCl, 2.5 mM MgCl2, 250 mM sucrose, 0.05% Nonidet P-40, 0.5% Triton X-100, 1 mM DTT, 1X protease inhibitor mixture) with 40U RNase OUT. Supernatant was incubated with mouse anti-V5 antibodies (Invitrogen) and equilibrated Gammabind-Plus resin slurry (GE Healthcare) for 3 h or overnight. Supernatant was collected for analysis, and beads washed 5 times in Lysis Buffer. 25% of the beads were used for protein analysis. The remainder was incubated for 2 h with

proteinase K. RNAs were extracted with phenol-chloroform-isoamyl alcohol, precipitated with glycogen in isopropanol, washed in 80% ethanol, resuspended in water and 3′labeled or analyzed by Northern blot.

For small RNA libraries, we established blasticidin-resistant S2 cell lines stably transformed with the pAWH-P19 or pAWH-NLS-P19 constructs, following the manufacturer instructions (Invitrogen). Fifteen 75cm2 plates with 80% confluent transformed cells were harvested, washed twice in PBS, and lysed at 4 °C for 1 h in Lysis buffer (see above), in the presence of equilibrated Gammabind-Plus resin for preclearing. After centrifugation (14000 × g, 15 min), 400 μl of Gammabind-Plus resin preloaded overnight in lysis buffer with 20 μg of high affinity rat anti-HA antibody (Roche #11867423001) were added to the supernatant and further incubated for 2 h at 4 °C. Beads were then washed five times in Lysis buffer supplemented to 800 mM NaCl. After proteinase K treatment, P19 or NLS-P19 associated RNAs were isolated by phenol/chloroform extraction and ethanol precipitated using carrier linear acrylamide.

RNA 3′ End Labeling. 10% of immunoprecipitated RNAs were incubated with 100 μCi pCp[5′,3′^{32}P] with 10U T4 RNA ligase (Roche) overnight at 4 °C. Unincorporated nucleotides were removed through G25 columns (GE Healthcare) or by ethanol precipitation with similar results. Samples were denatured 4 min at 95 °C and loaded onto 7M urea denaturing 15% polyacrylamide gel. 5′ labeled miR2a (GCTCATCAAAGCTGGCTGT-GATA, 23 nt), 3S18 (TTGCTATGTTTATGTTTATGTT-TATGC, 27 nt) oligos and Decade marker (Ambion) were used as size ladder. Signals were visualized by autoradiography. DNase I treatment of RNAs for 30 min at 37 °C followed by 10 min inactivation at 85 °C before labeling gave identical results.

Northern Blot Analysis. 20 μg of total RNAs isolated from transfected cells, or 90% of the immunoprecipitated RNAs were resolved by electrophoresis onto 7M urea denaturing 15% polyacrylamide gels. Northern blot analysis was performed in PerfectHyb Plus (Sigma) with sense 5′ ^{32}P end-labeled oligonucleotide probes. To detect siRNAs, probes were as follow: HMS-Beagle 5′-TCCCGACATTCCATAGGCATTTA-3′; roo 5′-TGGGCTCCGTTCATATCTTATG-3′. Membranes were hybridized at 37 or 38 °C overnight, washed for 5 min in 2× SSC, then twice 10′ in 2× SSC, 0.1% SDS. When necessary, membranes were stripped twice in boiling 0.1% SDS.

Western Blot Analysis. For protein analysis, equal amounts of proteins from each total extract, supernatant, or immunoprecipitate samples were boiled in Laemmli buffer and loaded on 15% SDS/PAGE. After transfer onto nitrocellulose membrane, Ponceau staining before Western blot analysis verified loading. Membranes were blocked in 5% milk, 1X PBS, 0.1% Tween, and incubated overnight with mouse HRP coupled anti-V5 antibody (1:5000, Invitrogen). Detection was performed using Supersignal Chemiluminescent Substrate (Pierce).

Informatic Analysis of Small RNA Libraries. Small RNA sequence files from our in house libraries were obtained and processed as fastq format files. Sequence reads were trimmed from the adapter sequence and matched to the *D. melanogaster* release 5.5 genome using novoalign (http://www.novocraft.com/). Only 19–29nt reads matching the genome with 0 or 1 mismatch were retained for subsequent analysis. For annotations, we used the release 5.5 fasta reference files available in Flybase, including a library of all transposon sequences (dmel-all-transposon r5.5.fasta), and the BDGP release 5.0 of miRNA sequences from Rfam (http://microrna.sanger.ac.uk/sequences). We used the compilation of transposable element canonical sequences (v9.4.1) from http://www.fruitfly.org/p disrupt/TE.html to determine the frequency table of individual TEs given in Fig. S3.

Sequence length distributions, small RNA mapping and frequency maps were generated using in-house Perl softwares to parse novoalign outputs (codes available on request). For small RNA mapping, we first matched each individual RNA sequence to the genome and gave to each matched position a weight corresponding to the occurrence of the sequence in the library divided by the number of genomic hits for the sequence (normalization). We then summed the values attributed to each position in a 5-kilobase sliding window and plotted this against the *Drosophila* chromosome maps using gnuplot. To determine the frequency maps of TE-matching small RNAs mapping to opposite genomic strands, we plotted the distance between each sequence read and its neighbors on the opposite strand over a −100 and +100 nt region. We obtained similar results with and without normalization of scores by the number of multiple genomic matches, indicating that these multiple matches do not skew the frequency maps over a 200 nt range.

1. Dunoyer P, Lecellier CH, Parizotto EA, Himber C, Voinnet O (2004) Probing the microRNA and small interfering RNA pathways with virus-encoded suppressors of RNA silencing. *Plant Cell* 16:1235–1250.
2. Rorth P (1998) Gal4 in the *Drosophila* female germline. *Mech Dev* 78:113–118.
3. Clegg NJ, et al. (1993) A cytogenetic analysis of chromosomal region 31 of *Drosophila* melanogaster. *Genetics* 134:221–230.
4. Brennecke J, Hipfner DR, Stark A, Russell RB, Cohen SM (2003) bantam encodes a developmentally regulated microRNA that controls cell proliferation and regulates the proapoptotic gene hid in *Drosophila*. *Cell* 113:25–36.

Fig. S1. B2, P19 and NLS-P19 suppress siRNA but not miRNA mediated silencing. (*A*) Flies expressing control GFP, B2, P19, or NLS-P19 under the control of the eye-specific GMR>GAL4 driver (*Upper*). An additional GMR>IR[w] transgene (*Lower*) triggers *white* RNAi resulting in lower eye pigmentation in the UAS>GFP control. *white* RNAi suppression is observed in B2 and P19 but barely detectable in NLS-P19 eyes. Corresponding relative eye pigment levels are shown on the right side. Error bars correspond to the standard deviation of three independent pigment level measurements (*B*) The GMR>GAL4 driver transgene triggers UAS-IR[EcR] expression in fly eyes where indicated. EcR RNAi results in the loss of corneal lens in flies expressing control GFP or NLS-P19, but is suppressed in flies expressing B2 or P19. (*C*) Confocal microscopy of wing imaginal discs expressing the *engrailed*-GAL4 driver in their posterior half compartment (P) and either a control *Tubulin*>GFP or a *Tubulin*>GFP-ban sensor with bantam miRNA target sites in 3′ UTR. The quadrant pattern of GFP silencing by bantam in the wing pouch (dashed lines) (4) is not affected by expression of B2, P19 or NLS-P19 in imaginal disc posterior compartment, indicating no obvious interference with the miRNA pathway by either viral protein.

Fig. S2. Expression of viral proteins in *Drosophila* cells. (*A*) Immunofluorescence on S2 cells transfected with empty vector (pMT), or constructs expressing V5 tagged B2, P19, or NLS-P19. After copper induction, B2 forms nuclear and cytoplasmic specks whereas NLS-P19 is found exclusively in the nucleus. P19 is very efficiently produced and localizes in the cytoplasm. DIC, differential interference contrast image; Blue, DAPI; red, α-V5. (*B*) Western blot analysis showing that transiently transfected V5-tagged viral proteins are efficiently immunoprecipitated (IP) from total cell lysates. Complete depletion of P19 from the supernatants (SN) could not be reached. (*C*) Western blot analysis showing that HA-tagged P19 and NLS-P19 expressed in stable cell lines (In) are efficiently immunoprecipitated (IP) from total cell lysates. Loading of the input samples (In) corresponds to one fifth of the IP samples (*D*) A sense roo probe revealed enriched siRNAs in Northern blots of P19 and NLS-P19 immunoprecipitates (IP) and longer RNA species (*) in B2 immunoprecipitate. I, corresponds to total RNA input material.

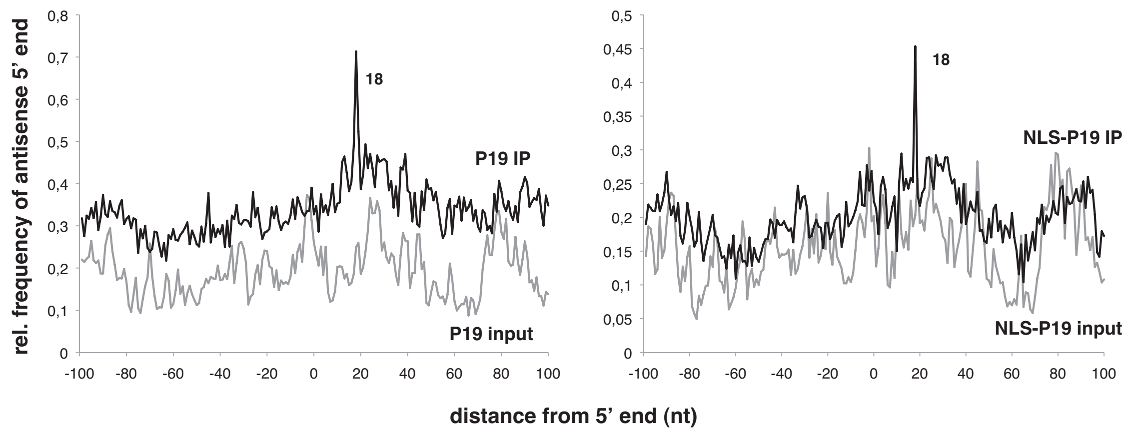

Fig. S3. Frequency maps, for the P19 input, P19 IP, NLS-P19 input and NLS IP libraries, of the separation of 297-matching siRNAs mapping to opposite genomic strands. The spike at position 18 indicates the position of maximal probability of finding the 5′ end of a complementary siRNA, which corresponds to a 19nt offset (graphs start at 0).

A

element	S2	P19 input	NLSP19 input	P19 IP	NLSP19 IP
297	18,68%	26,05%	28,10%	21,67%	28,73%
blood	17,00%	16,04%	15,60%	17,81%	15,97%
1731	12,45%	19,60%	19,74%	24,08%	20,72%
mdg1	7,85%	9,38%	10,75%	8,61%	7,56%
diver	6,93%	4,03%	3,61%	5,42%	2,36%
copia	4,89%	3,98%	3,14%	3,74%	5,85%
Juan	4,37%	2,34%	2,01%	2,11%	1,51%
jockey	3,66%	1,97%	1,95%	1,88%	1,30%
mdg3	3,62%	2,12%	1,54%	1,72%	1,28%
Bel-3S18	3,60%	1,46%	1,45%	1,27%	1,32%
Tirant	2,86%	1,23%	1,32%	1,84%	1,33%
roo	2,21%	2,53%	1,63%	2,23%	1,42%
micropia	2,06%	1,09%	1,25%	1,15%	2,06%
17.6	1,62%	1,72%	1,71%	1,87%	2,45%
Stalker2	0,56%	0,40%	0,40%	0,41%	0,34%

B

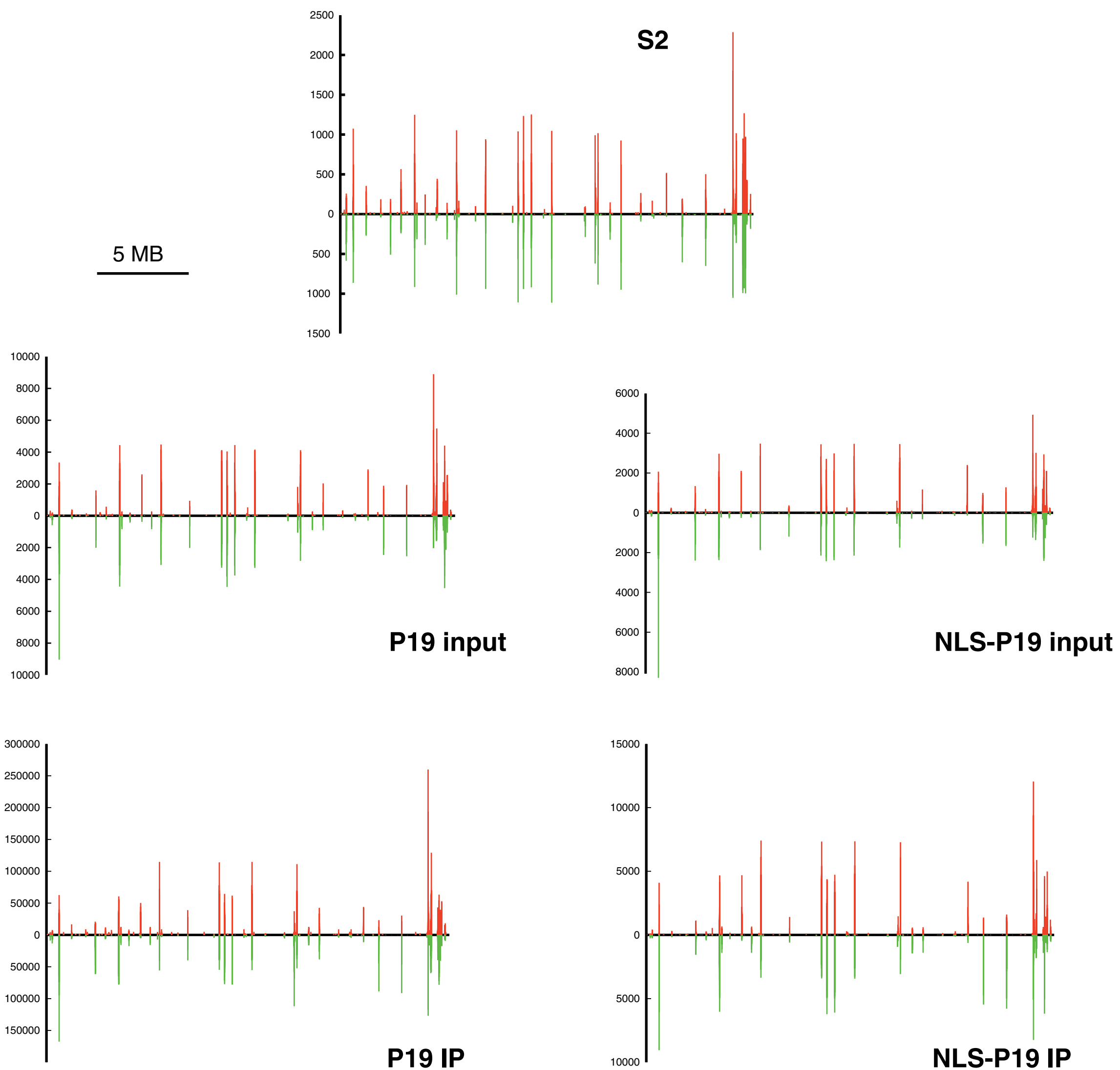

Fig. S4. Mapping of TE-derived siRNAs in S2, P19 input, P19 IP, NLS-P19 input and NLS-P19 IP libraries. (*A*) Heat map indicates the top-15 cloning frequencies for individual transposons in the five libraries. (*B*) Frequency maps of the TE-matching small RNAs from the five libraries on the chromosome X. The *x*- and *y*-axis represent the chromosomal position and the number of reads, respectively. The strand is represented by the color of the bars: plus (red) and minus (green).

Fig. S5. Expression of viral proteins in larval salivary glands. (*A*) Immunolocalization of viral proteins expressed in salivary glands using the lio-GAL4 driver. B2 is found in nucleoli, the nucleoplasm and the cytoplasm; P19 localizes in the cytoplasm and is enriched at the cytoplasmic membrane whereas NLS-P19 is restricted to the nucleus. Anti-FLAG: green; DAPI: red. (*B*) Western blot analysis probed with anti-FLAG and anti-alpha-tubulin antibodies showing B2, P19 and NLSP19 protein levels in male (m) or female (f) salivary gland extracts. Alpha-tubulin (50 kDa upper band) was used as loading control.

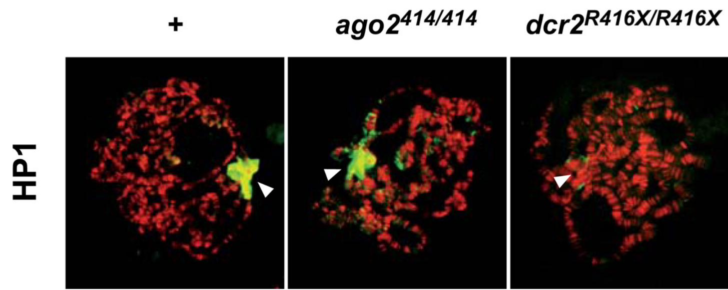

Fig. S6. *ago2* and *dcr2* mutations affect HP1 distribution. White arrowhead points to the chromosome pericentromere. Antibodies: green; DAPI: red.

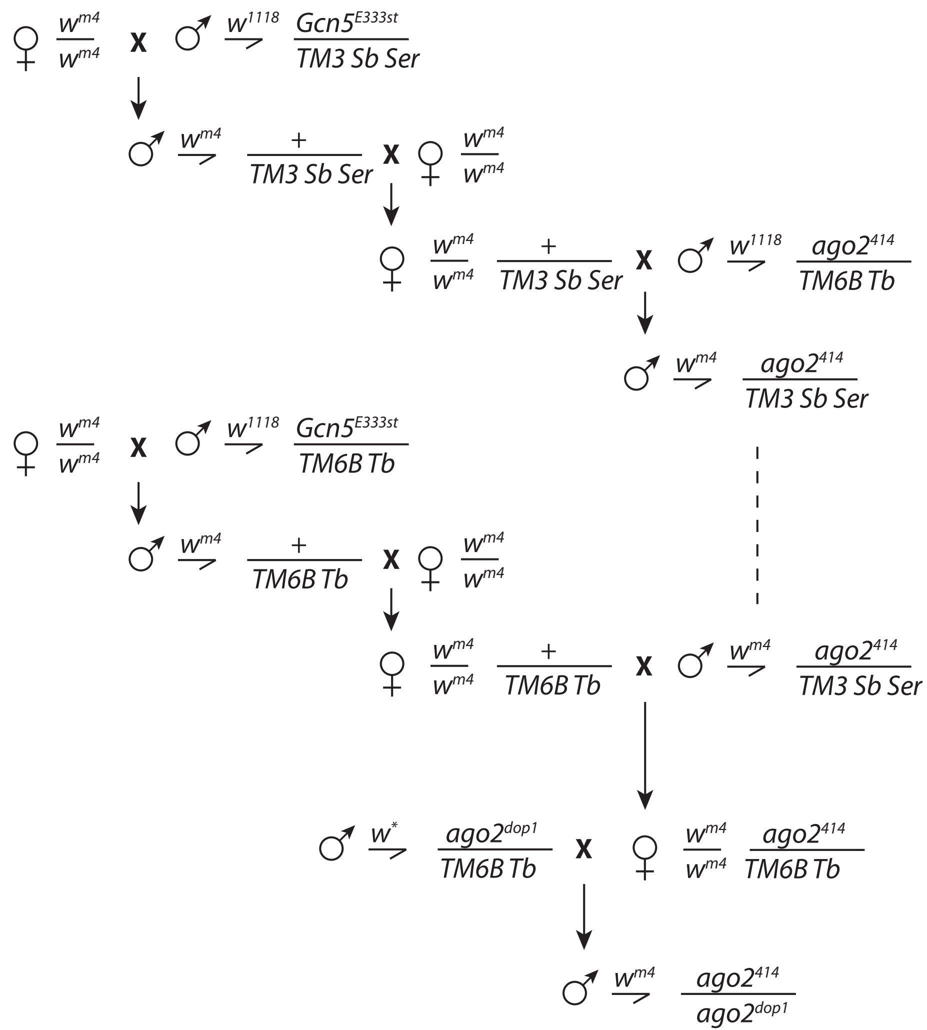

Fig. S7. Genetic crosses to generate RNAi mutant males bearing the *l (1)*w^{m4h} (w^{m4}) chromosome. Given is the genetic cross scheme to generate the w^{m4}/Y; $ago2^{414}/ago2^{dop1}$ heteroallelic combination presented in Fig. 5. Similar schemes were used for *dicer2* and *r2d2* mutant alleles, except that second chromosome GFP balancers *CyO* and *CyO* were used instead of the third chromosome balancers *TM3 Sb Ser* and *TM6B Tb*.

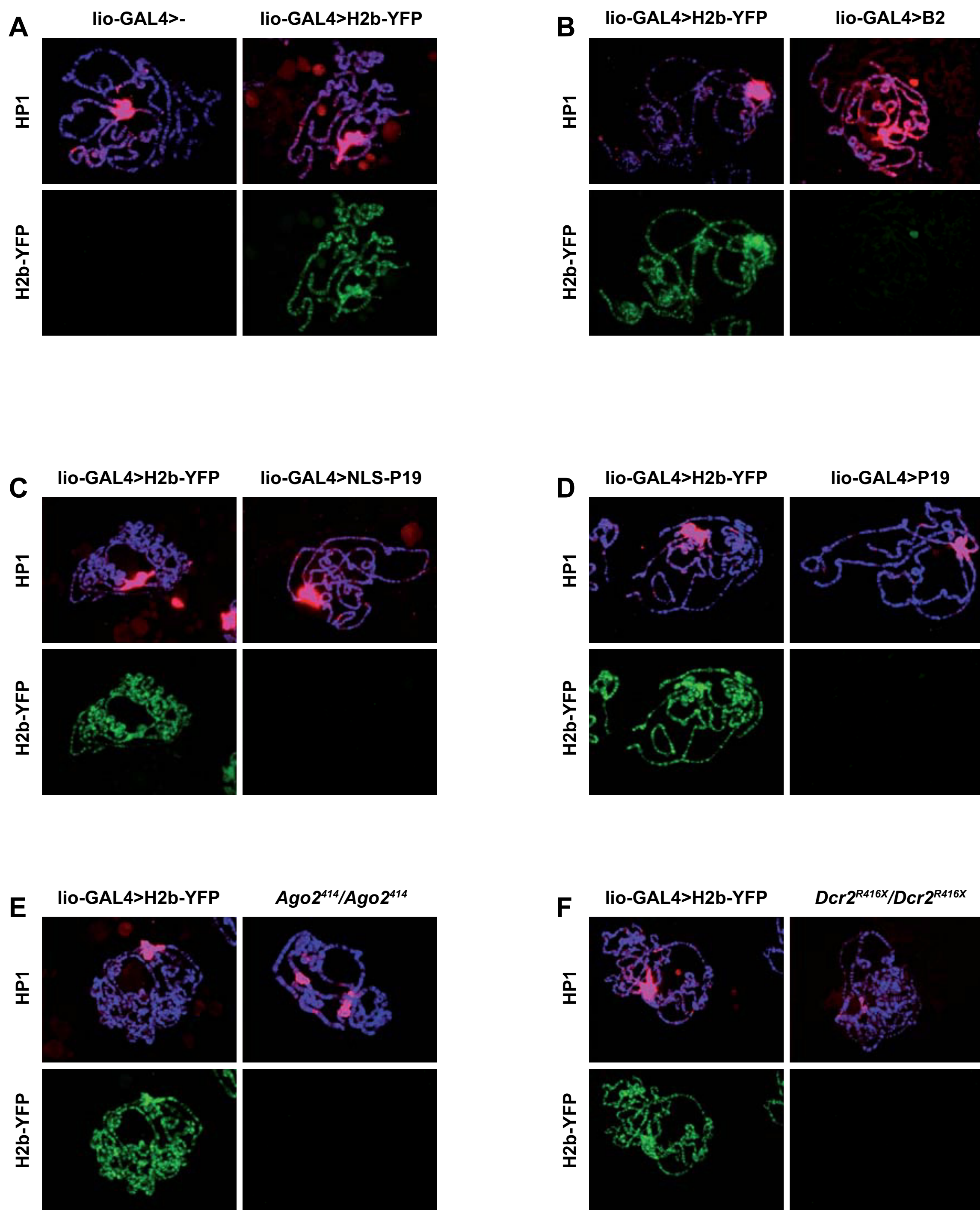

Fig. S8. B2, NLS-P19, *ago2* and *dcr2* mutations affect HP1 distribution on polytene chromosomes from third instar salivary glands. (*A*) Salivary glands from a *lio*>GAL4/+ and from a *lio*>GAL4/+; UAS>H2b-YFP/+ larvae were squashed on the same slide and stained with DAPI (blue) and anti-HP1 antibody (red). Chromosome sets were genotyped owing to yellow fluorescence of YFP. H2b-YFP expression does not affect HP1 distribution. Control salivary glands from *lio*>GAL4/+; UAS>H2b-YFP/+ (*Left*) and salivary glands from *lio*>GAL4/+; UAS>B2/+ (*B*), *lio*-GAL4/+; UAS>P19/+ (*C*), *lio*-GAL4/+; UAS>NLS-P19/+ (*D*), $ago2^{414}/ago2^{414}$ (*E*) or $dcr2^{R418X}/dcr2^{R418X}$ (*F*) larvae (*Right*) were spread on the same slide. Chromosome sets were stained and genotyped following the same procedure.